

From:
The Institute of Anatomy,
University of Bergen,
Norway.

A QUANTITATIVE ANALYSIS OF THE NUMERICAL DENSITY AND THE DISTRIBUTIONAL PATTERN OF PRISMS AND AMELOBLASTS IN DENTAL ENAMEL AND TOOTH GERMS

VI. THE VERTICAL COMPRESSION OF THE PRISM PATTERN ON THE OUTER ENAMEL SURFACE OF HUMAN PERMANENT TEETH

by

GISLE FOSSE

INTRODUCTION

In part IV the present author demonstrated the existence of a vertical compression of the prism pattern on the outer enamel surface of human permanent canines. By vertical is meant parallel to the longitudinal tooth axis.

Furthermore, the author demonstrated in part III that the distributional pattern of prisms in cross-section could be described by their centers. The contours of the separate prisms might assume the shape of arcades, hexagons or ellipses within the same pattern. The interprismatic substance might likewise vary in thickness within a homogeneous pattern.

Consequently, the calculated compression was not directly demonstrable in the form of the cross-sectioned prisms. However, *Eisenberg* (1938) had found that prism ends on the labial surface of incisors were quadrilateral, and recently *Hinrichsen* and *Engel* (1966) found that cross-sectioned prisms might show a flattened appearance. It is possible that these observations referred to a vertical compression of prism shape which was caused by the compression of pattern.

Several other authors have described or discussed the shape of prism in cross-section (*Hopewell-Smith*, 1926; *Chase*, 1927; *Merkel*, 1935; *Freiberg*, 1939; *Wolf*, 1942; *Helmcke*, 1963; *Boyde*, 1964; and *Romaniuk & Schraff*, 1965), but since none of them has explicitly distinguished between prism shape and the distributional pattern of prisms, it might be profitable to examine this relationship.

But the primary aim of this study was to examine the distributional pattern of prism rods which were sectioned transversally to their longitudinal axes. In the enamel of human teeth the prism rods usually run obliquely towards the outer surface in a longitudinal plane. Therefore the distributional pattern seen on the outer surface or in planes parallel to it does not represent the pattern of truly cross-sectioned prisms.

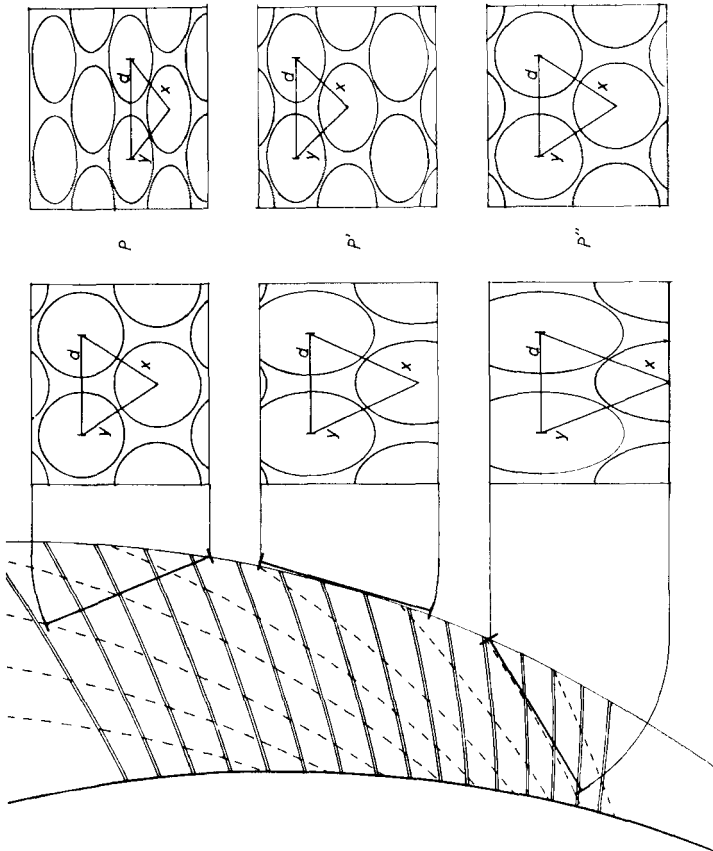


Fig. 1. The left part of the figure is a diagrammatic representation of a median tooth section. The stipled curves represent the Retzius lines, the double curves represent the main prism rod directions. The three straight lines which are at different angles to the tooth axis represent three section planes perpendicular to the median plane. The prism rod direction is perpendicular to the uppermost plane which is designed by the letter P. The middle plane, designated by P' is tangential to the outer surface. The lower plane designated by P'' is tangential to the incremental layers. The six squares illustrate the prism pattern in the three planes if the prisms are distributed in a symmetric hexagonal pattern in P, and if they are distributed in a symmetric hexagonal pattern in P''.

MATERIAL AND METHODS

A theoretical model

The left part of the drawing reproduced in Fig. 1 represents diagrammatically a median enamel section. The stipled curves represent the Retzius lines and the double curves represent the main prism rod direction. The three straight lines which are at different angles to the tooth axis represent three section planes which are perpendicular to the median plane. The uppermost plane which will henceforth be designated by P is orientated so that the prism rods are perpendicular to it. The middle plane, henceforth designated by P', is a tangent plane to the outer enamel surface. The lower plane is a tangent plane to the incremental layers and is designated by P". The angles between the prism rods, the Retzius lines and the outer enamel surface as represented in Fig. 1 are characteristic of human permanent enamel when sectioned longitudinally.

The three squares in the left-hand column of Fig. 1 illustrate diagrammatically the pattern of the cross-sectioned prisms in the respective planes if the prisms in P were distributed in a symmetric hexagonal pattern (where $d=y=x$, cf. part III). In P' and P" the transversal central distances designated by the letter d in the drawing, remain constant while y and x are elongated.

The three squares in the right-hand column illustrate the prism patterns if the distribution in P" were symmetrically hexagonal. In P and P' d remains unaltered while y and x have been shortened (K and K' being greater than 1.00, cf. part III).

[The sectioning of enamel in the P-planes

From human bicuspid and permanent molars a $600\ \mu$ thick median section from each tooth was cut in the Gillings sectioning machine. Each such median section was embedded in a plastic column with one of its cut surfaces in the upper surface of the column.

With the diamond point of the $25\times$ objective a line was ruled at an angle of 90° to the main prism direction in an area near the outer surface. A second line was ruled parallel to the incremental lines in the same area.

Fig. 2 is a photomicrograph from a median section of a bicuspid, representing an area near the buccal surface. The amelodentinal junction was below the area represented by the figure. The white line labelled P crosses the rods at an angle of 90° , while the line labelled P" runs parallel to the Retzius lines. The section marked thus was then cut along the P and P" lines perpendicularly to the upper surface of the column (cf. part V).

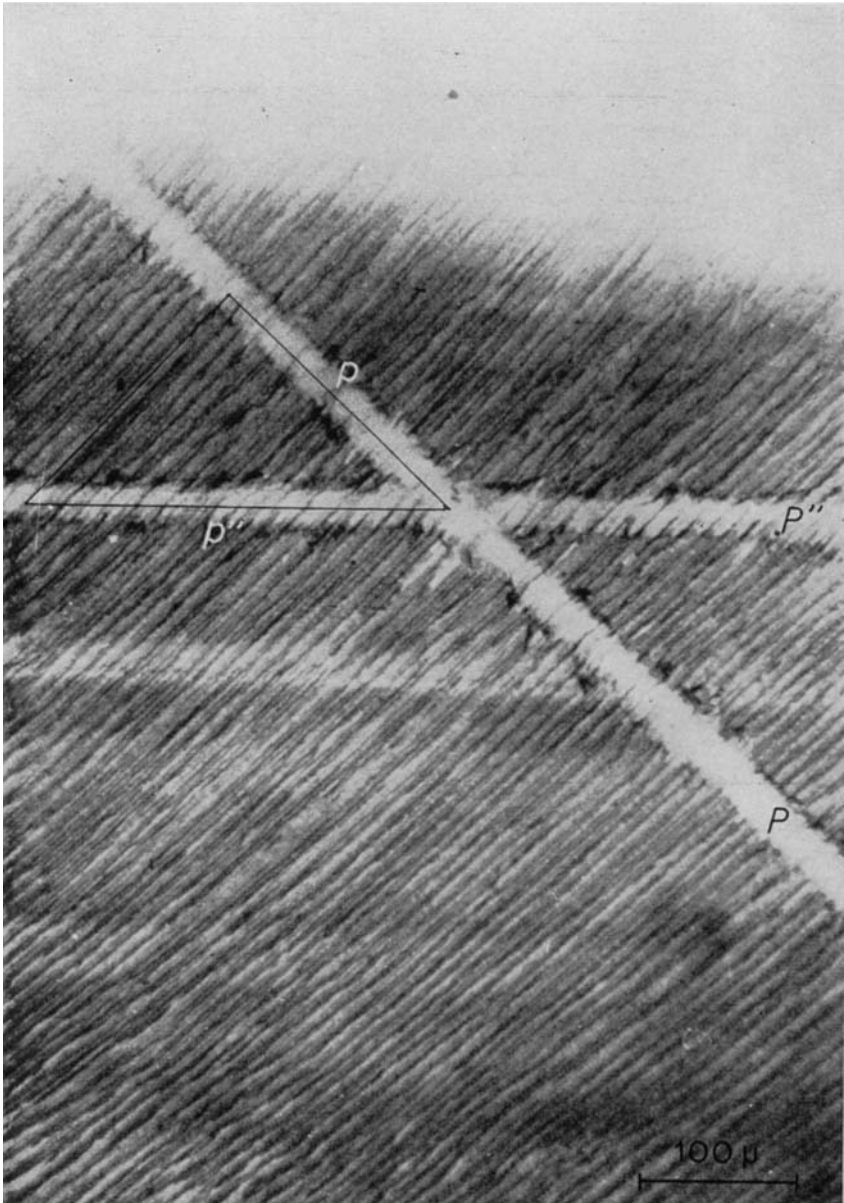


Fig. 2. Photomicrograph from a median section of a bicuspid representing an area near the buccal surface. The white line labelled P crosses the rods at 90°, while the line labelled P'' is parallel to the Retzius lines. The ratio between the hypotenuse p'' and the side p of the triangle approximates the compression ratio $\langle K \rangle$ in a section plane to which the prism rods are perpendicular.

Definition of the P and P'' planes in a median tooth section

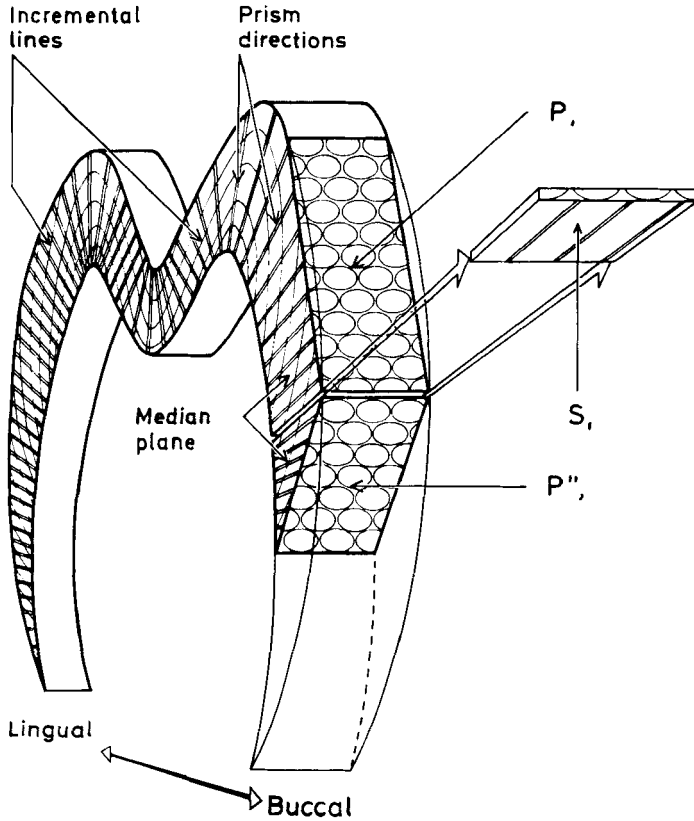


Fig. 3. A schematic representation of a median tooth section and the orientation of the P and P'' planes in relation to the prism rod direction and the incremental layers. The extracted plane designated by S is parallel to the prism rod direction.

The procedure outlined above was carried out for the buccal as well as the lingual surface on each median section.

The median section having been cut along the P and P'' lines was finally freed from the column by cutting in a plane planoparallel to the upper surface and 5 mm from this surface.

Fig. 3 is a diagrammatic drawing illustrating how such a median tooth section was cut along the lines labelled P and P" in Fig. 2. The two resultant section planes are called the P and P" planes and are accordingly labelled so in the diagram.

To verify that the prism rods were really parallel to the original median plane, the enamel was sectioned along the rod direction in the median plane through the point of intersection between the P and P" lines, in Fig. 2, and perpendicularly to the median plane. This was done after the P and P" planes had been photographed. In Fig. 3 is demonstrated the orientation of this section which is designated by S and whose photomicrograph is represented by Fig. 4. Along the left rim of the photograph is seen the median plane.

Microphotography of P and P" planes

Fig. 5 represents the P plane and Fig. 6 the P" plane of the area depicted by Fig. 2. These photographs were taken at a low magnification, using the 11 \times Leitz Ultropak objective. The intersection line between the planes is seen along the lower border of Fig. 5 and along the upper border of Fig. 6.

The photographs for direct measurements were taken by the 22 \times Leitz Ultropak objective. The regions photographed were situated near the intersection line and their longitudinal axes were aligned with the longitudinal axis of the tooth.

The calculation of prism density and pattern

In part III the author described his method of expressing the number of cross-sectioned prism per unit area and their distributional pattern by measuring the central distances between pairs of adjacent prisms within photographed enamel regions of a given area. In the present investigation the constant area of the regions was 26.817 μ^2 .

In this paper the regional prism density is expressed by the $\langle \text{agr} \rangle$ -value and the standard deviation S_{agr} .

The prism pattern and its variation are described by the values of $\langle K \rangle$ and the standard deviation S_K . $\langle K \rangle$ is a ratio expressing the degree of vertical compression of the prism pattern. By vertical in this connection is meant a direction in a plane through the longitudinal axis of the tooth.

For each region the means of the three central distances symbolized by $\langle d \rangle$, $\langle y \rangle$ and $\langle x \rangle$ are given. In a system of hexagonally distributed points these symbols signify the central distances in the three main directions.



Fig. 4. Prism rods sectioned longitudinally in an S plane from the median section represented by Fig. 2. The orientation of the S plane in relation to the median section is illustrated in Fig. 3.



Fig. 5. The P plane of the median section represented by Fig. 2. This photomicrograph was taken by the $11\times$ Leitz Ultropak objective. The intersection line between this plane and the P'' plane is seen along the lower border.

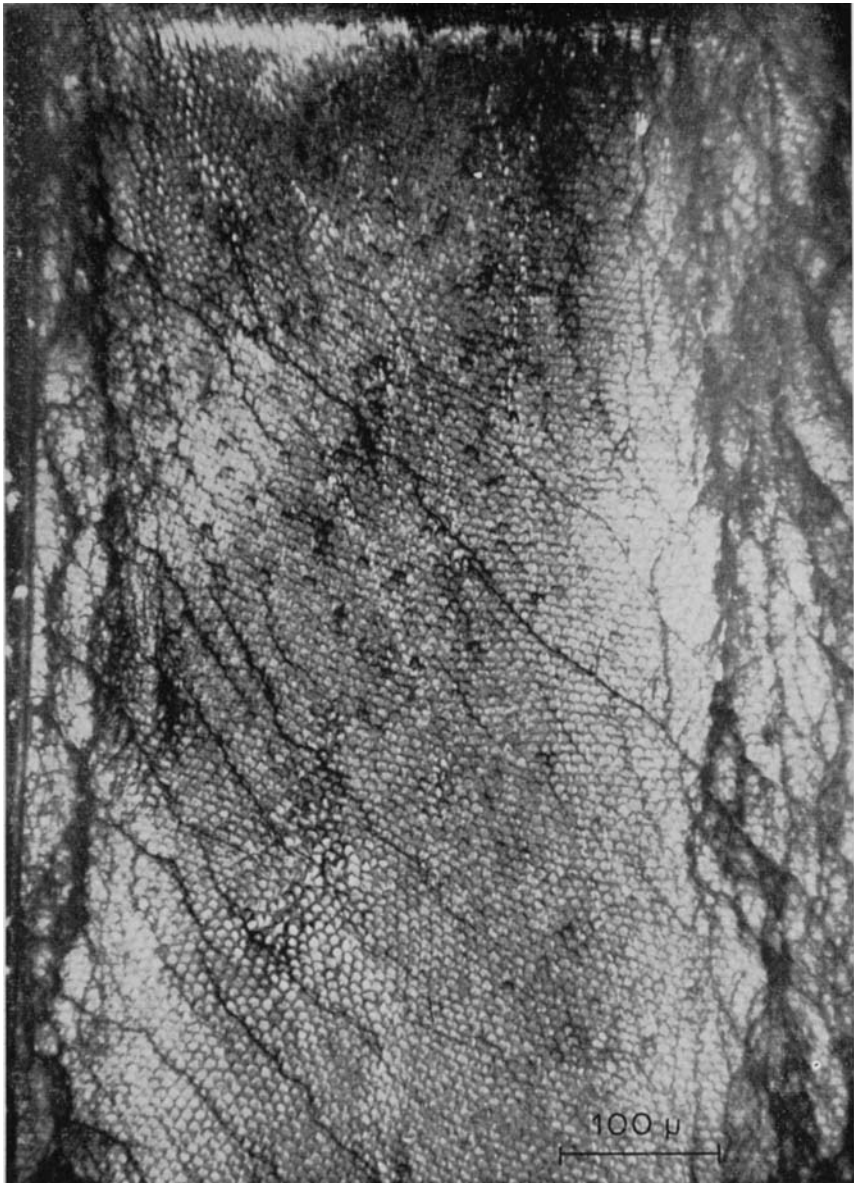


Fig. 6. The P'' plane of the median section represented by Fig. 2. The intersection line between this plane and the P plane is seen along the upper border. The photomicrograph was taken by the $11\times$ Leitz Ultropak objective.

Table I.
Density, central distances and compression ratios of prisms in the P- and P''-planes on the buccal and lingual surfaces of 4 different teeth.

Tooth no.	Tooth surf.	Section plane	Groups	Prisms/mm ² (agr)	Triangles Sagr	Centr. distances			Vertical compress.				
						<d>	<y>	<x>	K	SK	$\frac{\langle K \rangle}{\langle K \rangle'}$	$\frac{P''}{P}$	
1. (molar)	Bucc.	P	10	28276	2044	110	7,71	6,10	5,97	1,46	0,20	1,56	1,33
		P''	8	16454	1197	72	8,06	8,01	9,73	0,93	0,16		
	Ling.	P	9	29331	2040	122	7,71	6,07	5,84	1,55	0,56	1,39	1,46
		P''	9	16738	976	78	8,60	8,62	7,86	1,11	0,19		
2. (canine)	Bucc.	P	6	31406	878	78	6,84	5,94	5,65	1,30	0,22	1,25	1,31
		P''	9	21352	1732	97	7,46	7,33	7,35	1,04	0,14		
	Ling.	P	7	28037	1989	84	7,53	6,14	5,96	1,42	0,22	1,44	1,42
		P''	9	19169	1547	96	7,75	7,65	8,15	0,98	0,14		
3. (bicuspid)	Bucc.	P	10	30440	1150	150	7,13	5,76	5,93	1,35	0,18	1,16	1,38
		P''	9	20589	1249	104	8,06	7,93	6,81	1,16	0,19		
	Ling.	P	10	28882	2715	101	7,65	5,63	6,25	1,46	0,20	1,55	1,53
		P''	10	17542	3224	55	7,92	8,07	8,95	0,94	0,17		
4. (bicuspid)	Ling.	P	10	29254	3133	126	7,62	6,11	5,85	1,46	0,22	1,37	1,62
		P''	9	19614	1339	102	7,87	6,88	8,83	1,06	0,16		
											Mean:	1,38	1,43

RESULTS

Fig. 7 represents a region of the P plane, and Fig. 8 represents a region of the P" plane from the buccal area represented by Fig. 2. The specimen was a bicuspid.

Fig. 9 represents the P' plane while Fig. 10 represents the P" plane of the lingual surface of a permanent molar.

In Table I are listed the means of the three central distances, the $\langle \text{agr} \rangle$ -values with their standard deviations, the $\langle \text{K} \rangle$ -values with their standard deviations and in the second last column the ratio between the $\langle \text{K} \rangle$ -values for each pair of planes. The denominator is the $\langle \text{K} \rangle$ -value from the P" plane. The table contains the values from 4 different teeth, including the bicuspid and the permanent molar represented by Figs. 7 to 10.

The ratios in the last column will be explained in the next chapter.

Testing of theory against present and previous findings

It is seen from the table that in all the P" planes $\langle \text{K} \rangle$ is either greater or smaller than the value 1.00, while there is a marked compression in the P planes, higher than was found on the outer surface of the enamel mantle of human permanent canines (cf. part IV).

t-tests were carried out between the $\langle \text{K} \rangle$ -values of the P and P" planes and the probability that the samples were from the same K-universe was always below the 0.1 % level.

This compression is also plainly visible in the photomicrographs represented by Figs. 7 and 9. The results seem to conform with the distributional pattern outlined in the right column of the diagram in Fig. 1.

In Fig. 2 a right-angled triangle has been drawn. The hypotenuse lies in the P" line and one of the sides in the P line, while the other side lies in the rod direction.

The hypotenuse is called p", while the side in P is designated by p.

According to the general definition of K, $\frac{p''}{p} = \frac{\text{K}}{\text{K}}$, in a model where all rods are mathematical prisms. In Table I the $\frac{p''}{p}$ ratios for different areas are listed in the last column. There seems to be a certain conformity between these ratios and the corresponding $\frac{\langle \text{K} \rangle}{\langle \text{K} \rangle''}$ ratios.

The compression ratio on the outer enamel surface may be symbolized by $\langle \text{K} \rangle'$. If the compression ratio in the P" plane equals 1.00, then $\langle \text{K} \rangle'$ equals the ratio between the length of the Retzius line intersected by two

parallel separate rods and the length of the outer surface intersected by the same rods if they were mathematical prisms. Fig. 11 represents a segment of the median plane of C_1 , a human permanent canine where the prism density and compression had been measured in numerous positions on the outer enamel surface. The ratio between the intersected Retzius line and the outer surface approximates 1.30 in the area depicted in Fig. 11. This area corresponds to reg. 15 on C_1 , where $\langle K \rangle = 1.32$ (cf. part IV, Table II).

Fig. 12 represents the median plane through region 2 of the same tooth. The ratio between the Retzius line and the outer surface approximated 1.28. The $\langle K \rangle$ -value on the outer surface in region 2 was 1.27 (cf. part IV, Table IV). However, the ratio between the Retzius line and the outer surface, in position 13, equalled 1.17 while $\langle K \rangle$ equalled 1.10. The difference was even greater in position 7 where the ratio was 1.00 while $\langle K \rangle$ equalled 1.23.

On C_1 therefore, the $\langle K \rangle$ -values in the P'' planes would hardly be found to equal 1.00 in positions 13 and 7.

In the depth series of C_1 (cf. part V) there seemed to be a gradual decrease of $\langle K \rangle$ -values towards the value 1.00 near the amelo-dentinal junction in places where there had been an actual increase of enamel surface during amelogenesis. This will mean that near the dentine $\langle d \rangle$ was smaller than $\langle y \rangle$ or $\langle x \rangle$ in section planes planoparallel to the incremental layers.

If it is assumed that the distributional pattern of ameloblasts in cross section planoparallel to the ameloblastic layer is symmetrically hexagonal near the outer enamel surface, and that each ameloblast produces one prism rod, then the prisms will be flattened in cross sections perpendicular to their long axes, whenever these axes are inclined to the ameloblastic layer. This flattening or compression of pattern must occur in the same direction as that to which the rods incline.

Fig. 13 is a diagrammatic representation of this phenomenon. The ameloblasts are drawn perpendicularly to a P'' plane, and the prisms which are inclined to the left, are sectioned transversely to their long axes by a P plane. The cross section of the prisms in the P plane will be the geometric projection of the ameloblasts in the P'' plane. The distance labelled h will equal $H \sin \alpha$, α being the acute angle between prism rod and ameloblastic layer. This angle would thus be identical to the acute angle between prism rods and Retzius lines in longitudinal tooth sections.

If the ameloblasts during their outward motion are displaced in other than the centrifugal direction, the orientation of their long axes being unaltered, a changed shape of the prism rods will ensue.

Fig. 14 is a photomicrograph from a longitudinal section of a human tooth germ. The ameloblasts are seen in the upper right corner. Incremental lines

parallel to the ameloblastic layer are seen in the enamel matrix. Some of these lines seem to be caused by abrupt changes of prism rod direction in the section plane.

Fig. 15 represents the matrix of the same section, photographed by a higher magnification using oil immersion.

Apparently the transverse prismatic diameter increases at the bends of the rods. This is in agreement with the theory since the diameter of the rods parallel to the ameloblastic layer should remain constant over shorter distances if the number of ameloblasts remains constant and if each ameloblast produces one prism rod.

Fig. 16 represents a longitudinal section from the mature enamel of a dog's permanent canine. The rods run perpendicularly to the Retzius lines that lie almost parallel to the outer enamel surface which is seen along the upper rim of the photograph. In a previous investigation the author did not find any vertical compression of the prism pattern on the outer surface of a dog's permanent canine (cf. part V, Tables I, II, III and IV).

DISCUSSION

If the incremental layers are the original sites of the ameloblastic layer, if the ameloblasts are distributed in a symmetric hexagonal pattern and if each ameloblast produces one prism rod, then the prism pattern must be compressed in the P planes as was demonstrated by the findings presented in this paper.

On the other hand the flattening of prism rods when inclined to the incremental or ameloblastic layer is hardly conceivable if the number of prism rods were independent on the number of productive ameloblasts in a given area. In the latter case the cross-sectioned prisms would rather be expected to appear as was depicted diagrammatically in the left-hand column of Fig. 1.

The findings presented in this paper demonstrated that the vertical compression found on the outer surface of human permanent enamel needs not be caused by an actual lateral distension of the ameloblastic layer, manifesting itself by greater d values than y and x values in this layer. However, since there was little or no compression near the amelodontal junction in human enamel, (cf. part V), one cannot conclude from the present findings that the vertical compression is solely caused by the angle between rods and the ameloblastic or incremental layer.

Hypothetically one may conclude that at the beginning of amelogenesis the ameloblasts are distended in a vertical direction. If there is a positive surface growth of enamel during amelogenesis this vertical distension is

gradually reduced towards the outer surface until the ameloblasts are distributed in a regular symmetric hexagonal pattern at the conclusion of amelogenesis.

Since the distributional pattern of cross-sectioned prisms has not been dealt with systematically before, it is difficult to compare the present results with observations made by earlier authors.

However, *Eisenberg* (1938) had observed that prism ends on the labial surface of incisors were quadrilateral. *Hinrichsen* and *Engel* (1966) had observed that cross-sectioned prisms sometimes showed a flattened appearance.

These observations may refer to the vertical compression that certainly seems to lead to a flattened rectangular shape of the prisms, see Figs. 7 and 9.

Wolf (1942) and *Boyde* (1964) stated that the prisms assume an arcade shape when their course towards the ameloblastic layer is oblique. *Romaniuk* and *Schraff* (1965) believed that prisms are arcade shaped or polygonal when they approach the outer surface at an acute angle. Excepting the flattening of prisms, which is a secondary effect caused by the compression of pattern, the present author has not considered the primary influence of the angle between rods and incremental layers on prism shape. This possible influence and its effects do not directly concern the findings presented in this paper.

CONCLUSIONS

Near the buccal and lingual outer surface of the enamel of human permanent teeth, the prism rods when sectioned in planes planoparallel to the incremental layers, tend to be distributed in a symmetric hexagonal pattern. Therefore, when sectioned perpendicularly to their long axes, the prism rods are distributed in a pattern which is compressed vertically. The arcades in such cross-sections have a very flattened, rectangular shape.

This compression may theoretically be expressed as $\frac{1}{\sin \alpha}$ where α is the acute angle between prism rods and Retzius lines in the median plane of the tooth.

SUMMARY

From each of 4 human permanent teeth, a molar, a canine and two bicuspids, was cut a 600 μ thick median section. In a small region near the outer enamel surface of a median section the enamel was sectioned in one plane perpendicular to the rod direction, and in a second plane planoparallel to the incremental layers.

On each median section, one such pair of section planes was prepared on the buccal surface, and one on the lingual surface.

In each region the two section planes were compared concerning prism pattern, density and shape.

In all planes perpendicular to the rod direction the pattern was markedly compressed in a vertical direction. The prisms had a flattened rectangular arcade shape and the horizontal diameters were visibly greater than the vertical diameters.

In the section planes planoparallel to the incremental layers, the pattern was symmetrically hexagonal, the prisms having a «normal» arcade shape.

Photomicrographs were presented to illustrate these findings, and the numerical values of the prism density and vertical compression in the two section planes of each region were presented in a table.

Accepting that the incremental layers in the mature enamel are the original sites of the ameloblastic layer, the author presumed that whenever the rods are inclined to the ameloblastic layer they assume a flattened shape in cross section, if at the same time the ameloblasts are distributed in a symmetric hexagonal pattern. The direction of this compression then coincides with the direction of the inclination.

The author felt that the flattening of prism rods when inclined to the ameloblastic layer was incomprehensible without assuming that each ameloblast is responsible for one prism rod.

The degree of vertical compression on the outer enamel surface, discovered by the present author and described by him, is a function of the angles between prism rods, the Retzius lines and the outer enamel surface in median sections, and is not caused by an actual lateral distension of the ameloblastic layer.

Still the vertical compression in the outer layers of human enamel may be caused by the surface growth of enamel, since this compression was not manifest near the amelodontinal junction (cf. part V). The author, therefore, presumed that at the beginning of enamel formation in human permanent teeth, the ameloblastic layer is distended vertically. This vertical distension is then gradually reduced towards the final outer enamel surface.

RÉSUMÉ

LA COMPRESSION VERTICALE DE LA DISPOSITION DES PRISMES À LA SURFACE EXTERNE DE L'ÉMAIL DE DENTS PERMANENTES HUMAINES

Quatre dents permanentes humaines, une molaire, une canine et deux prémolaires ont servi à la préparation d'une coupe médiane de 600 μ d'épaisseur pour chacune de ces dents.

Dans une région limitée située près de la surface externe de l'émail de la coupe médiane, l'émail a été taillé suivant un plan perpendiculaire à la direction des prismes, et suivant un second plan parallèle au plan des couches incrémentales.

Sur chaque coupe médiane, une paire de ces deux sortes de plans de coupe a été préparée sur la face vestibulaire, et une autre paire sur la face linguale.

Dans chaque région, les deux plans de coupe ont été comparés en ce qui concerne la disposition des prismes, leur densité et leur forme.

Dans tous les plans perpendiculaires à la direction des prismes, la disposition était nettement comprimée dans le sens vertical. Les prismes avaient une forme aplatie en arcade rectangulaire, et les diamètres horizontaux étaient nettement plus grands que les diamètres verticaux.

Dans les plans de coupe parallèles au plan des couches incrémentales, la disposition était hexagonale et symétrique, les prismes ayant une forme en arcade «normale».

L'auteur présente des microphotographies illustrant ces observations, et des tableaux indiquant les valeurs numériques de la densité prismatique et de la compression verticale dans les deux plans de coupe de chaque région.

Admettant que les couches incrémentales de l'émail à maturité représentent les endroits où la couche améloblastique était placée primitivement, l'auteur suppose que, dans les cas où les prismes sont inclinés sur la couche améloblastique, ils présentent une forme aplatie sur les coupes transversales si la répartition des améloblastes présente en même temps une disposition hexagonale symétrique. La direction de cette compression coïncide alors avec la direction de cette inclinaison.

Pour l'auteur, l'aplatissement des prismes lorsqu'ils sont inclinés sur la couche améloblastique reste incompréhensible si l'on ne suppose que chaque améloblaste est responsable d'un prisme.

Le degré de la compression verticale à la surface externe de l'émail, découverte par l'auteur et décrite par lui, est fonction des angles formés par les prismes, les lignes de Retzius et la surface extérieure des couches des coupes médianes, et n'est pas causé par une véritable distension latérale de la couche améloblastique.

Pourtant, la compression verticale dans les couches superficielles de l'émail humain peut être causée par la croissance de la surface de l'émail, puisque cette compression n'était pas observée près de la jonction émail-dentine (voir partie IV). L'auteur suppose donc qu'au début de la formation de l'émail des dents permanentes humaines, la couche améloblastique est distendue dans le sens vertical. La distension verticale diminue ensuite progressivement en allant vers la surface extérieure finale de l'émail.

ZUSAMMENFASSUNG

DIE VERTIKALE KOMPRESSION DES PRISMENMUSTERS AUF DER ÄUSSEREN FLÄCHE DES SCHMELZMANTELS DER MENSCHLICHEN BLEIBENDEN ZÄHNE
 Von jedem von vier menschlichen bleibenden Zähnen, einem Molaren, einem Eckzahn und zwei Prämolaren, wurde ein $600\ \mu$ dicker Medianschnitt ausgeschnitten.

In einer kleinen Region dicht bei der Schmelzoberfläche von einem solchen Medianschnitt wurde der Schmelz in einem Plan senkrecht zur Prismenrichtung, und in einem Plan planparallel zu den »Retziusplänen«, geschnitten.

Auf jedem Medianschnitt wurde ein Paar von solchen Schnittplänen auf der buccalen Fläche präpariert, und ein Paar auf der lingualen Fläche.

In jeder Region wurden die zwei Pläne verglichen, bezüglich Prismenmusters, Prismendichtheit und Prismenform.

In allen Plänen senkrecht zur Prismenrichtung war das Prismenmuster deutlich in eine vertikale Richtung komprimiert. Die Prismenquerschnitte hatten eine flache, rektanguläre Arcadenform, und die horizontalen Durchmesser waren sichtbar grösser als die vertikalen Durchmesser.

In den Schnittplänen die planparallel zu den »Retziusplänen« waren, war das Prismenmuster symmetrisch hexagonal; die Querschnitte der Prismen hatten eine normale Arcadenform.

Mikrophotographien illustrierten diese Funde, und die numerische Dichtigkeit und die vertikale Kompression der Prismen in den zwei Plänen jeder Region wurden in einer Tabelle dargestellt.

Wenn es vorausgesetzt wird, dass die Retziuslinien die Spüre der Ameloblastenschichten zu verschiedenen Zeitpunkten der Amelogenese seien, nahm es der Verfasser an, dass wenn die Prismen schräg zu der Ameloblastenschicht laufen, werden sie flach im senkrechten Querschnitt, wenn auch die Ameloblasten in einem symmetrischen hexagonalen Muster verteilt seien. Die Richtung dieser Kompression sei dann dieselbige wie die der Neigung der Prismen zur Ameloblastenschicht.

Die Kompression der Prismen schien dem Verfasser unerklärlich ohne anzunehmen, dass jeder Ameloblast für ein Prisma verantwortlich sei.

Die Grösse der vertikalen Kompression auf der äusseren Fläche des Schmelzmantels, entdeckt und beschrieben von diesem Verfasser, ist eine Funktion von den Winkeln zwischen Prismen, Retziuslinien und der Schmelzoberfläche in Medianschnitten, und ist nicht von einer wirklichen lateralen Ausdehnung der Ameloblastenschicht verursacht.

Doch möchte die vertikale Kompression in den äusseren Schichten des Schmelzmantels vom Oberflächenwachstum des Schmelzmantels verursacht

sei, darum, dass diese Kompression dicht bei der Schmelz-Dentingrenze nicht beobachtet werden konnte (cf. Teil V). Daraus schliesst der Verfasser, dass im Anfang der Amelogenese der menschlichen bleibenden Zähne, die Ameloblastenschicht vertikal ausgedehnt sei. Diese vertikale Ausdehnung sei dann allmählich gegen die endliche Oberfläche des Schmelzmantels reduziert.

REFERENCES

- Boyde A.*, 1964: The structure and development of mammalian enamel. Thesis. Depart. of Anat. The London Hosp. Med. Coll., London. In stensil.
- Chase S. W.*, 1927: The enamel prisms and the interprismatic substance. *Anat. Rec.* 36: 239—258.
- Eisenberg M. J.*, 1938: A microscopic study of the surface enamel of human teeth. *Anat. Rec.* 71: 221—226.
- Freiberg K.*, 1939: Über die Gestalt der Schmelzsäulen. *Z. Zellforsch.* 29: 390—404.
- Gustafson A. G.*, 1959: A morphologic investigation of certain variations in the structure and mineralization of human dental enamel. *Odont. T.* 67: 361—472.
- Hinrichsen C. F. L. & M. B. Engel*, 1966: Fine structure of partially demineralized enamel. *Arch. Oral. Biol.*, 11: 65—93.
- Hopewell-Smith A.*, 1926: Concerning human enamel; Facts, explanations and applications. *Dent. Cosmos*, 68: 639—667.
- Merkel E.*, 1935: Über die Gestaltung der Schmelz-Dentingrenze und die Form der Schmelzprismen in menschlichen Zähnen. Inaugural. Dissert. in Breslau, Akad. Diss. 1935.
- Romaniuk K. & F. R. Schraff*, 1965: Directional variation in the terminal portions of the enamel rods in human deciduous teeth. *J. Dent. Res.* 44: Suppl. New Zealand Abstr. 1208.
- Wolf J.*, 1942: Der Einfluss der Ameloblastenverschiebungen auf die Gestalt und den Verlauf der Schmelzprismen. *Dtsch. Zahn-, Mund- u. Kieferheilk.* 9: 488—522.

Address:

*The Institute of Anatomy,
University of Bergen,
Norway*

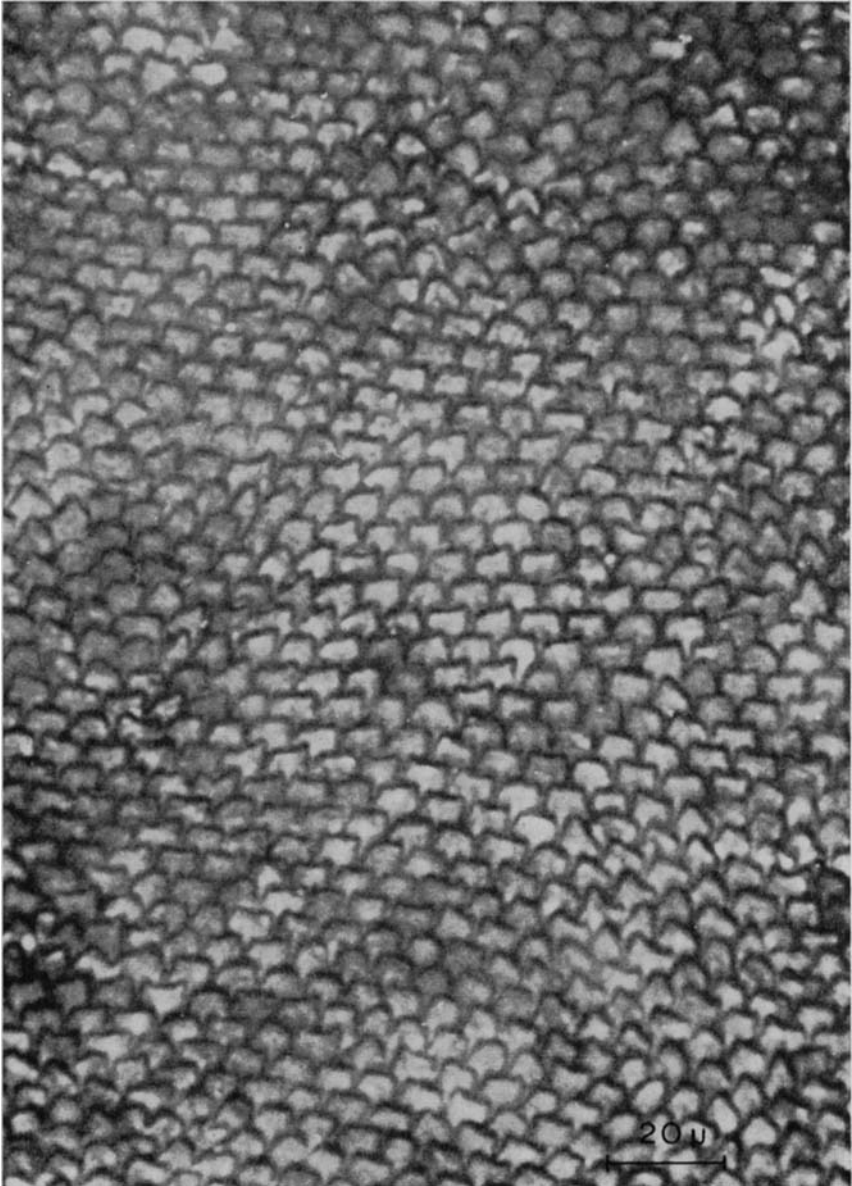


Fig. 7. The P plane of the median section represented by Fig. 2. Photomicrograph taken by the $22\times$ Leitz Ultropak objective.



Fig. 8. The P'' plane of the median section represented by Fig. 2.
22 \times Leitz Ultropak objective.

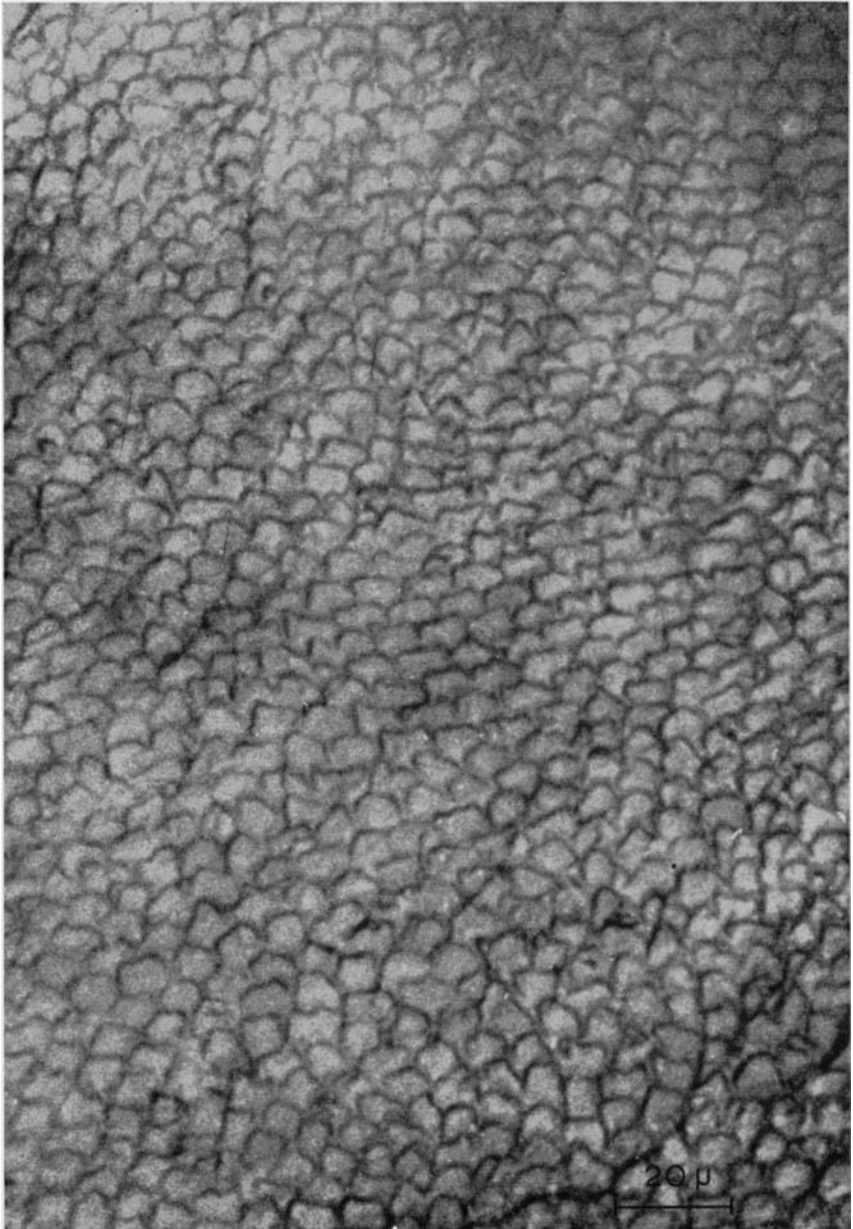


Fig. 9. The P plane of the lingual surface of a molar.
22 × Leitz Ultropak objective.

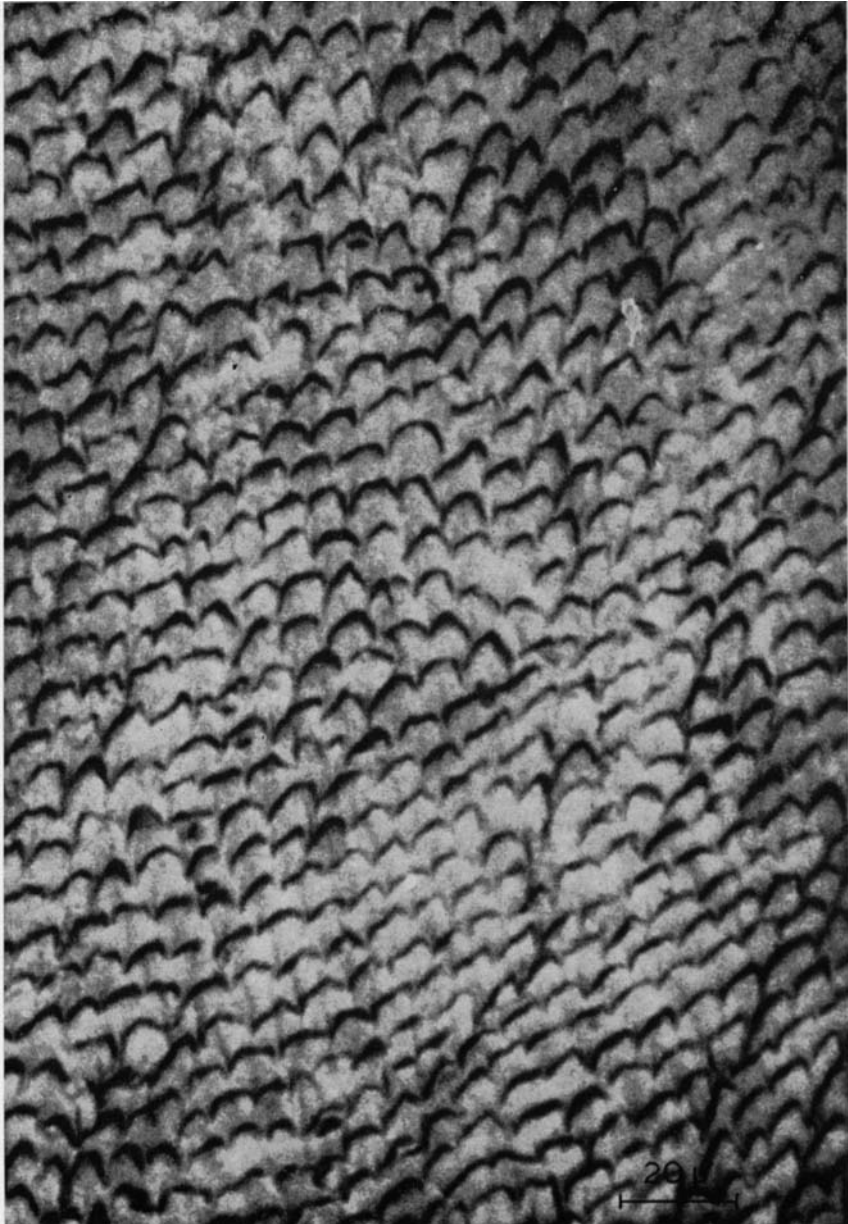


Fig. 10. The P' plane of the lingual surface of a molar.
22 × Leitz Ultropak objective.



Fig. 11. Position 15 of the median section of C_1 , a human permanent canine, with the guide line following the main prism rod direction.



Fig. 12. Position 2 of the median section of C₁ with the guide line.

The compression of the prisms as a function of the angle between the prism rods and the ameloblastic layer.

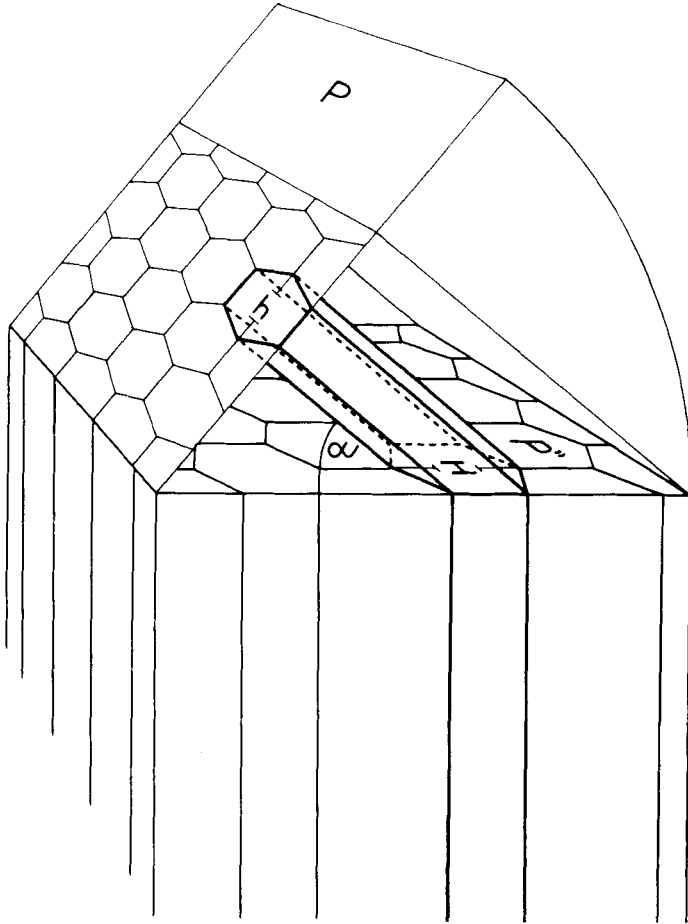


Fig. 13. A schematic representation of the vertical compression of the prisms as a function of the angle between the prism rods and the ameloblastic layer. This angle is designed by α , the vertical height of the ameloblasts by H and the resultant vertical height of the prisms in the P plane by h .

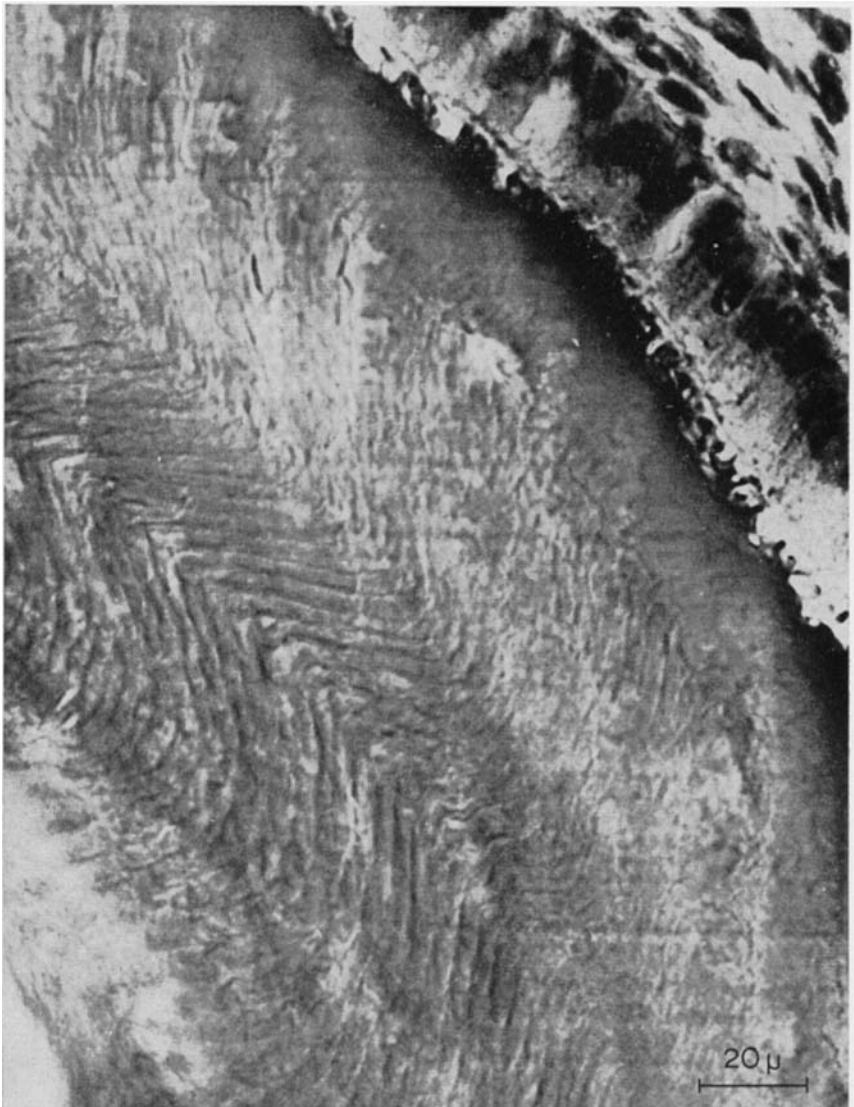


Fig. 14. A median section through the enamel matrix and the ameloblasts of the tooth germ of a human deciduous central incisor. Some of the Retzius lines are caused by sharp bends in the prism rods.

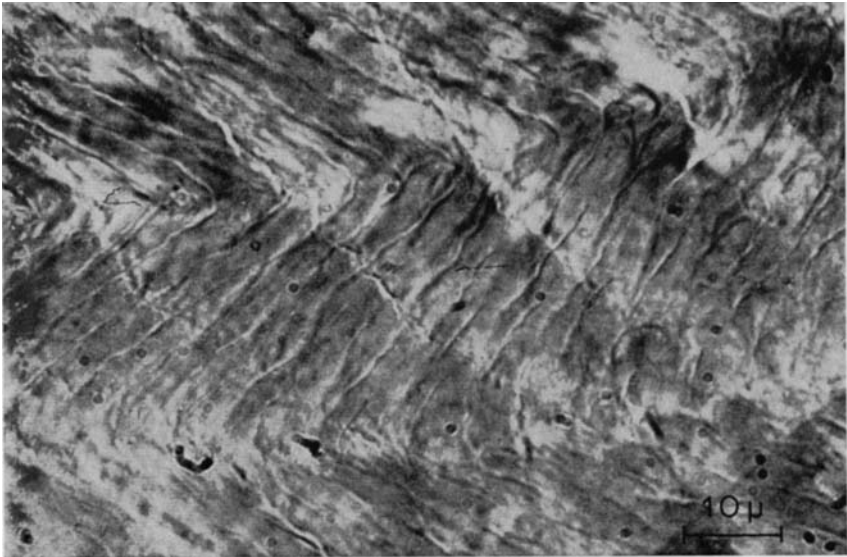


Fig. 15. The prism rods in the matrix of the median section represented by Fig. 14. The rods seem thicker where they change direction. $100\times$ Leitz oil immersion objective.

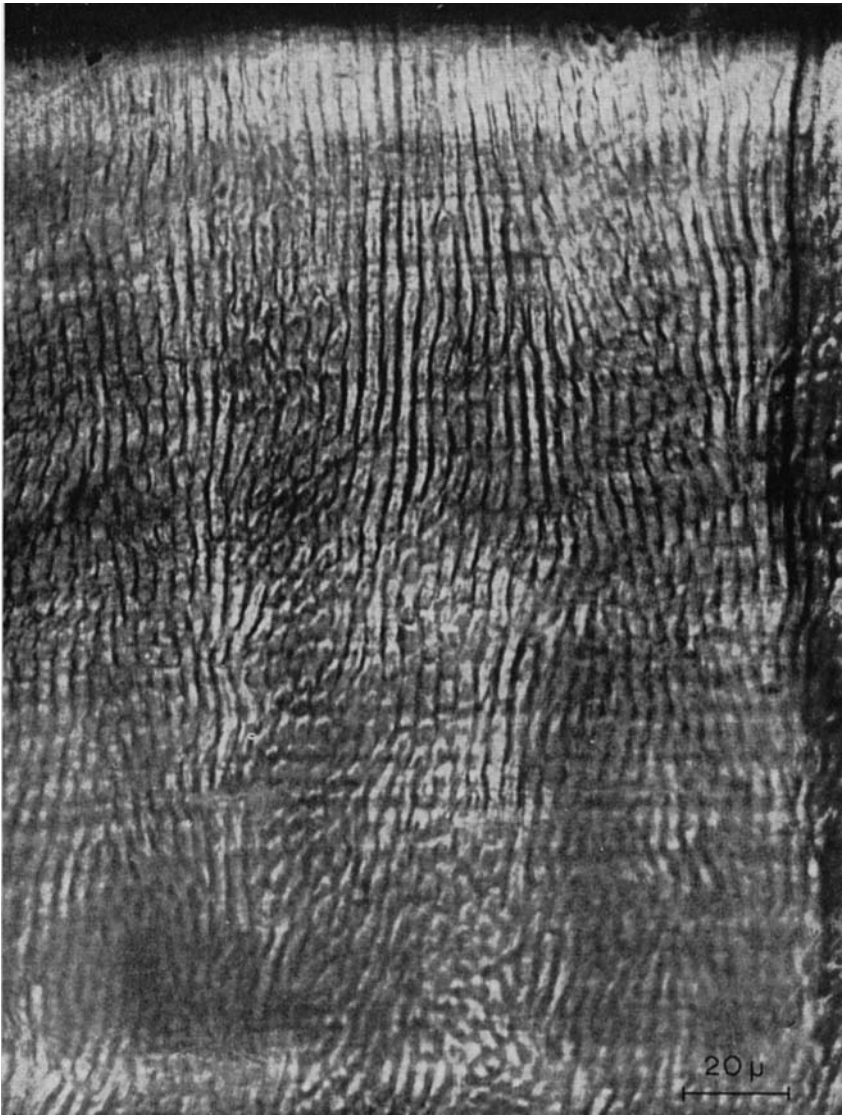


Fig. 16. Prism rods in a median section of a dog's permanent canine. The prism rods are nearly perpendicular to the outer enamel surface which is seen along the upper border. The Retzius lines are practically parallel to the outer surface.